

Uncertainty Analysis of a Landmark Initialization Method for Simultaneous Localization and Mapping

Henry Huang, Frederic Maire and Narongdech Keeratipranon

Faculty of Information Technology
Queensland University of Technology
Box 2434, Brisbane Q 4001, Australia

Email: {h5.huang@student., f.maire@, n.keeratipranon@student.}qut.edu.au

Abstract

To operate successfully in any environment, mobile robots must be able to localize themselves accurately. In this paper, we describe a method to perform *Simultaneous Localization and Mapping* (SLAM) requiring only landmark bearing measurements taken along a linear trajectory. We solve the landmark initialization problem with only the assumption that the vision sensor of the robot can identify the landmarks and estimate their bearings. Contrary to existing approaches to landmark based navigation, we do not require any other sensors (like range sensors or wheel encoders) or the prior knowledge of relative distances between the landmarks. We provide an analysis of the uncertainty of the observations of the robot. In particular, we show how the uncertainty of the measurements is affected by a change of frames. That is, we determine what can an observer attached to a landmark frame deduce from the information transmitted by an observer attached to the robot frame. This SLAM system is ideally suited for the navigation of domestic robots such as autonomous lawn-mowers and vacuum cleaners.

1 Introduction

Any spatial relationship between the objects of interest in the environment of a robot will be called a *Map*. One of the fundamental challenges in mobile robotics is the *Simultaneous Localization and Mapping* (SLAM) problem. A SLAM system builds incrementally a map of an unknown environment from observations made by the robot. To predict the robot location, conventional SLAM systems rely on odometric measurements [Russell and Norvig, 2003; Siegwart and Nourbaksh, 2004]. Unfortunately, the accumulation of odometric errors (due mainly to wheel slippage) make the accuracy of position estimations based only on odometry worsen rapidly. Other sensors are needed if the robot navigates for a long time. The determination of an estimate of the posi-

tions of the landmarks is known as the *Landmark Initialization* problem. An accurate landmark initialization is essential to solve the SLAM problem.

Solutions to SLAM when the mobile robot is equipped with sensors that provide both range and bearing measurements to landmarks are well developed [Leonard and Durrant-Whyte, 1991; Zunino and Christensen, 2001]. The navigation systems of commercially available autonomous lawnmowers rely on sensors measuring the magnetic field created by a perimeter wire [RoboMower, 2005; Toro, 2005]. Some experimental systems work with more expensive sensing devices, like differential GPS or laser tracking systems that help locate the mowers exactly within a meter exist, but are considered too expensive for domestic robots. Due to advances in computer vision, cameras are becoming popular alternative sensors for SLAM because of their lower cost, weight and power consumption. SLAM systems using only vision include [Kwok and Dissanayake, 2004; Costa *et al.*, 2004; Sola *et al.*, 2005; Lemaire *et al.*, 2005].

Landmark bearings can be obtained with an omnidirectional vision sensor (for example, a camera aiming at a catadioptric mirror). An omnidirectional image is radial with the camera position at its centre. Although it is not straightforward to obtain range measurements from the image due to the shape of the mirror, the bearings of landmarks relative to the robot are reasonably accurate and easy to derive from the image [Rizzi and Cassinis, 2001; Yagi *et al.*, 1998; Delahoche *et al.*, 1997]. In [K. Usher and Corke, 2002], an omnidirectional vision sensor was installed on a Toro ride-on mower, and landmark bearings were retrieved directly from the radial images to navigate the mower.

In [Huang and Maire, 2004], landmark bearings derived from panoramic views taken from a set of random *observation points* (points from where the observations are made) are used by an iterative search method to induce the positions of the landmarks (this method requires three or more landmarks). The search is performed by minimizing a distortion error which measures the inconsistency between the observations and the hypothesized positions of the landmarks. The method that we propose in this paper does not require an it-

erative search, but directly computes the relative Cartesian coordinates of the landmarks and the observation points. The only extra requirement that we make is that the robot should be able to move in a straight line and make observations to extract the bearings of the landmarks.

In general, vision sensors are noisy. Dealing with sensory noise and uncertainty is essential in robotics navigation. Robustness to noise in the sensors can be achieved with probabilistic methods such as *Extended Kalman Filters* (EKF) [Smith *et al.*, 1990; Dissanayake *et al.*, 2001] or Particle Filters [Montemerlo and Thrun, 2003].

In this paper, we call a *Landmark Frame* (denoted by \mathcal{F}_L), a Cartesian coordinate reference system attached to two distinguished landmarks. If we assume that all landmarks are stationary, then \mathcal{F}_L is a *Global Frame*. Ultimately, we wish to estimate the positions of all objects in this global frame. Our proposed method is particularly efficient for dealing with uncertainty and solves the problem of global localization in SLAM. The *Uncertainty Region* of an object is the set of possible points that are consistent with the observations made by the robot. This region/area for a landmark L_i will be denoted by \mathcal{A}_{L_i} .

The rest of the paper is structured as follows. Section 2 reviews related works on bearing-only SLAM, in particular the landmark initialization problem. Section 3 describes our approach. In Section 4, we present experimental results on the sensitivity of the system to noise. Finally, in Section 5, we discuss future work.

2 Related work

For localization the robot needs to know where the landmarks are, whereas to estimate the positions of landmarks the robot needs to know where it is on the map. The problem of map-building is considered as a chicken-and-egg problem [Siegwart and Nourbaksh, 2004]. Without initialization of the landmarks, the robot location can be predicted by EKF with odometric measurements. EKF requires the knowledge of the previous pose of the robot. The common approach assumes that the initial position of the robot is at the origin of the *Robot Frame* (robot centred frame). Landmark positions can thus be estimated by the predicted robot positions and sensory measurements. [Davison, 2003] uses a separate Particle Filter to estimate the distance from the observation point to the landmark with a single camera. The estimated distance is not correlated with other observations due to the limitation of the field of view. The follow-up work in [Davison *et al.*, 2004] improves the SLAM results by applying a wide-angle vision camera. In [Bailey, 2003], past poses of the robot are stacked in the memory to perform landmark initialization. Once the landmarks are initialized, the batch of observations is used to refine and correct the whole map. [Costa *et al.*, 2004] presents an iterative solution to the landmark initialization of bearing-only SLAM problem with *unknown data association* (all landmarks are visually identical). The authors

estimate the landmark positions via Gaussian probability density functions that are refined as new observations arrive.

Landmark initialization based on memorizing previous measurements or iterative methods cause time delay for estimation. They belong to the *delayed* landmark initialization methods [Sola *et al.*, 2005]. Some immediate initialization methods of bearing-only SLAM called *undelayed* landmark initialization were introduced in [Kwok and Dissanayake, 2004; Sola *et al.*, 2005]. [Kwok and Dissanayake, 2004] presents a multiple hypotheses approach to solve the problem in a computationally efficient manner. Each landmark is initialized in the form of multiple hypotheses distributed along the direction of the bearing measurement. The validity of each hypothesis is then evaluated based on the *Sequential Probability Ratio Test* (SPRT). [Sola *et al.*, 2005] gives a new insight to the problem and presents a method by initializing the whole cone that characterizes the direction of the landmark. This cone is covered by a sequence of ellipses that represent the likelihood of the landmark.

Undelayed landmark initialization is an efficient method to identify the directions of all landmarks when the first bearing measurements are made. It does not state explicitly the locations of the landmarks, hence further observations are required to initialize the landmark positions. The method introduced in [Sola *et al.*, 2005] is not a pure bearing-only method as it requires the minimum and maximum range of vision. [Lemaire *et al.*, 2005] applies an undelayed initialization method into practical 3D bearing-only SLAM problem. The landmark initialization is similar to the method proposed in [Kwok and Dissanayake, 2004] (maintain a mixture of Gaussians). The updating process is done by comparing the likelihoods of subsequent observations. If the likelihood falls below a certain threshold then the Gaussian is removed. Once only a single Gaussian is left in the cone, the landmark is initialized and added into the map for EKF-SLAM.

[Huang *et al.*, 2005] presents a localization system with two observations from a linear trajectory, each observation contains only the bearing measurements of two landmarks. It is a global localization method and does not rely on odometry. The estimated uncertainty depends on the relative difference in bearings. The uncertainty is proportional to the distance from the observation point to the landmark. Similar conclusions are reported in [Kwok *et al.*, 2004] where a path planning strategy for bearing-only SLAM is presented. Proper path planning and landmark selection are essential to improve SLAM.

We propose a similar approach of undelayed landmark initialization. However, instead of using a sequence of Gaussians to cover the uncertainty cone, we manipulate directly each cone as a polyhedron. Each cone contains a landmark (see Figure 1). Another observation is still required to initialize the landmark. After a second observation, the uncertainty region of the landmark becomes the intersection of two cones rooted at the two observation points (see Figure 2). Depend-

ing on the difference of bearings, the intersection is either a quadrangle (four-side polygon) or an unbounded polyhedron.

For each estimation from a linear trajectory, we transfer the robot centered observations into the global frame \mathcal{F}_L (see Section 3 for details). The uncertainty regions of all objects are re-computed with respect to the landmark frame during the change of bases. A global map with the estimated positions of all objects and their associated uncertainty regions can be gradually built this way while the robot explores its environment.

3 Our approach

In this section, we show how to estimate the relative positions of some landmarks L_1, L_2, \dots, L_n from landmark bearings taken by a robot at two observation points R_1 and R_2 (we assume that the robot is moving in a linear trajectory with unknown distance as shown on Figure 2).

Once the landmarks are initialized, to localize the robot position in the environment becomes fairly straightforward. In order to describe our method we need to introduce some notation.

The landmark frame \mathcal{F}_L is determined by the landmarks L_1 and L_2 . More precisely, L_1 is the origin and by definition $\|L_1 - L_2\| = 1$. That is $\|L_1 - L_2\|$ is taken as the measurement unit. We define also a *robot frame*, denoted by \mathcal{F}_R . The frame \mathcal{F}_R is a robot centred frame; R_1 is its origin and R_2 is by definition at $[1 \ 0]'$. In other words, the distance $\|R_1 - R_2\|$ is taken as the measurement unit in \mathcal{F}_R .

We denote \mathcal{B}_i^j the bearing measurement of the i^{th} landmark with respect to the robot heading direction at the j^{th} observation point. The uncertainty region/area of L_i is denoted by \mathcal{A}_{L_i} .

Assume that the error range for the bearings is $\pm\epsilon$. At an observation point R_j , the landmark position L_i is contained in the cone which is formed by two rays rooted at R_j . The first ray is defined by R_j and the bearing $\mathcal{B}_i^j + \epsilon$; the second ray is defined by R_j and bearing $\mathcal{B}_i^j - \epsilon$. Figure 1 shows the cones in the robot frame \mathcal{F}_R based on the reading of the landmark bearings from R_1 .

After reading the bearing measurements from both R_1 and R_2 , the uncertainty region \mathcal{A}_{L_i} becomes the intersection of two cones rooted at R_1 and R_2 respectively. Figure 2 shows a typical situation (bounded intersections). If the cones are almost parallel, their intersection can be an unbounded polyhedron.

The spatial relationships in Figure 2 are expressed in the robot frame \mathcal{F}_R . Since the robot is moving over time, its frame changes too. Therefore, it is necessary to change coordinate systems to express all positions in the global frame \mathcal{F}_L . Figure 3 illustrates the difficulty of expressing the robot centered information in the global frame \mathcal{F}_L . The uncertainty on the landmarks prevents us from applying directly a change of bases. In the next Section, we will show how to address this problem.

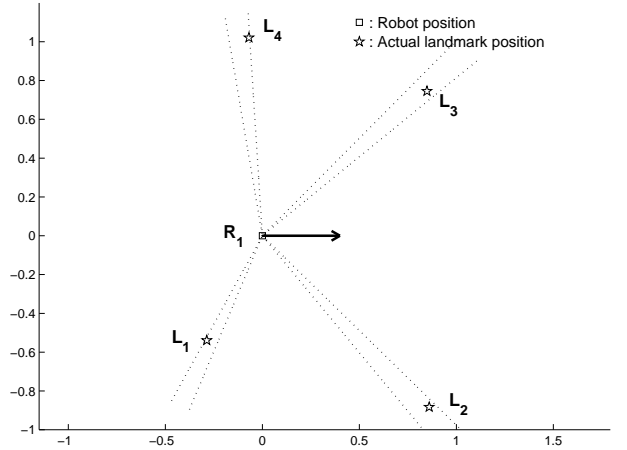


Figure 1: The cones rooted at the first observation point R_1 contain the landmarks. Each cone represents the uncertainty of the bearing of the associated landmark. The diagram is drawn with respect to the robot frame \mathcal{F}_R .

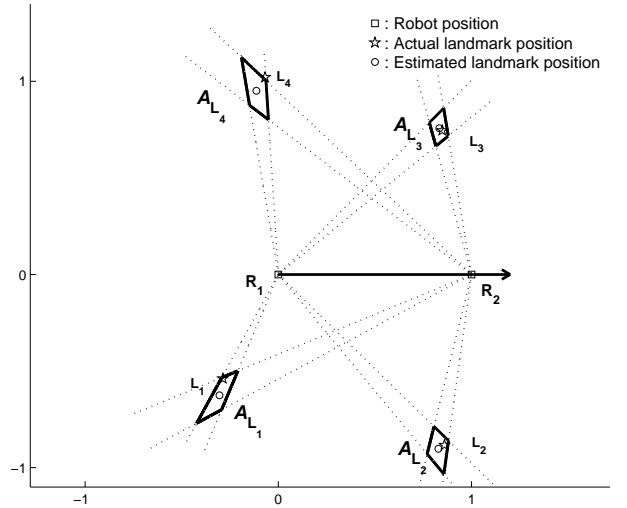


Figure 2: The intersections of the cones form the uncertainty regions \mathcal{A}_{L_i} .

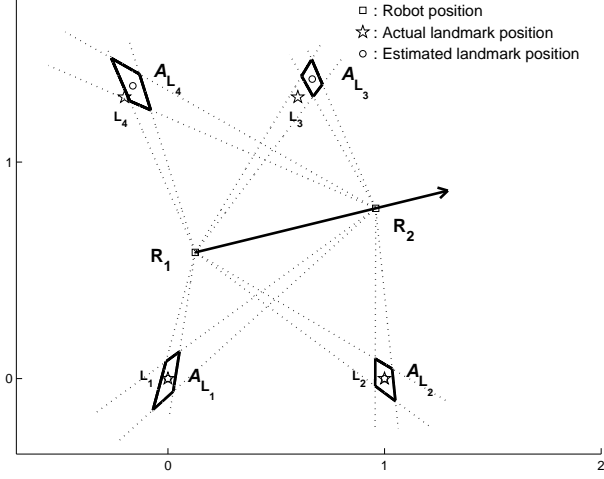


Figure 3: If the uncertainty regions of the landmarks are each reduced to a point, a simple change of bases is sufficient to express the robot centered information in the landmark frame \mathcal{F}_L . If the uncertainty regions of the landmarks are larger, the transfer of information is more complicated.

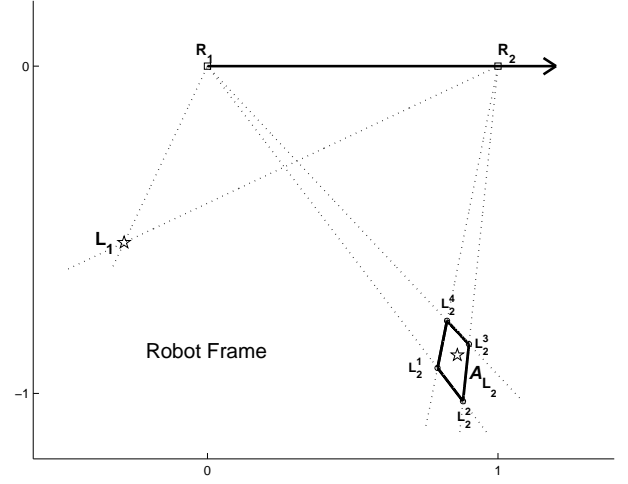


Figure 4: In \mathcal{F}_R , the uncertainty region of L_2 is \mathcal{A}_{L_2} . The four vertices of \mathcal{A}_{L_2} are denoted by $L_2^k, k = 1 \dots 4$.

3.1 Uncertainty and change of frames

From the noisy observations made in the robot frame \mathcal{F}_R , we would like to derive the uncertainty regions of the observed objects with respect to the landmark frame \mathcal{F}_L .

Given a point M , $X_R(M)$ denotes the coordinate vector of M in frame \mathcal{F}_R ; and $X_L(M)$ denotes the coordinate vector of M in frame \mathcal{F}_L .

Consider the simple case of Figure 4 which contains only two landmarks and two robot positions. Assume the robot (the observer) sees L_1 clearly from R_1 and R_2 , but sees L_2 with some uncertainty. The uncertainty region of L_1 in \mathcal{F}_R is reduced to a single point (no ambiguity). Whereas, the uncertainty region of L_2 in \mathcal{F}_R is a polyhedron.

The uncertainty regions of R_1 and R_2 with respect to \mathcal{F}_L can be obtained by considering all possible hypotheses for the location of L_2 consistent with the observations. That is, we consider the set of possible coordinate vectors $X_R(L_2)$ of L_2 in \mathcal{F}_R . For each hypothesis $X_R(L_2) = h_2$, a standard change of bases returns the coordinates $X_L(R_1)$ and $X_L(R_2)$ of respectively R_1 and R_2 with respect to \mathcal{F}_L . Making h_2 range over the vertices of \mathcal{A}_{L_2} in Figure 4, create the polyhedra \mathcal{A}_{R_1} and \mathcal{A}_{R_2} of uncertain regions with respect to \mathcal{F}_L (see Figure 5).

In the general case, when uncertainty exists for both L_1 and L_2 , to transfer the information from \mathcal{F}_R to \mathcal{F}_L , we consider simultaneously all the possible locations of L_1 and L_2 consistent with the observations. We hypothesize,

$$X_R(L_1) = h_1, \text{ and } X_R(L_2) = h_2 \quad (1)$$

Let $\mathcal{T}_{(h_1, h_2)}$ be the affine transformation function for

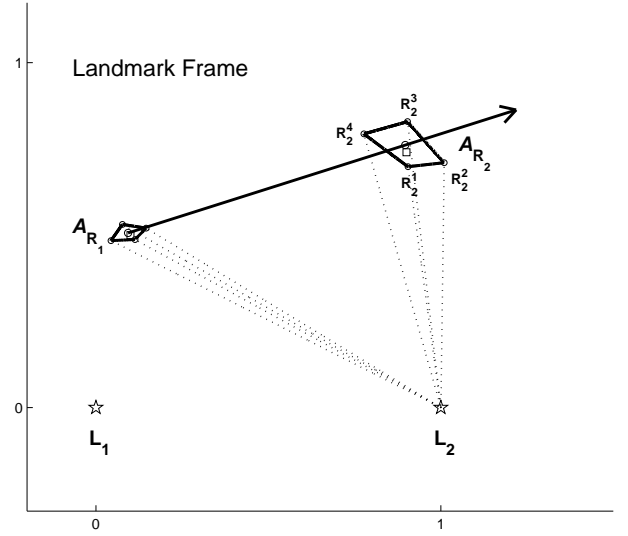


Figure 5: After the change of frames, the uncertainty areas of R_1 and R_2 are denoted by \mathcal{A}_{R_1} and \mathcal{A}_{R_2} . R_2^k is obtained from Equation 4 with respect to L_2^k in \mathcal{F}_R , where $k = 1 \dots 4$.

changing frames from \mathcal{F}_R to \mathcal{F}_L . That is,

$$X_L(L_1) = \mathcal{T}_{(h_1, h_2)}(X_R(L_1)) = [0 \ 0]' \quad (2)$$

$$X_L(L_2) = \mathcal{T}_{(h_1, h_2)}(X_R(L_2)) = [1 \ 0]' \quad (3)$$

The above constraints completely characterize $\mathcal{T}_{(h_1, h_2)}$. For any point M , the information transfer between the two frames is done with Equation 4.

$$X_L(M) = \mathcal{T}_{(h_1, h_2)}(X_R(M)), \quad (4)$$

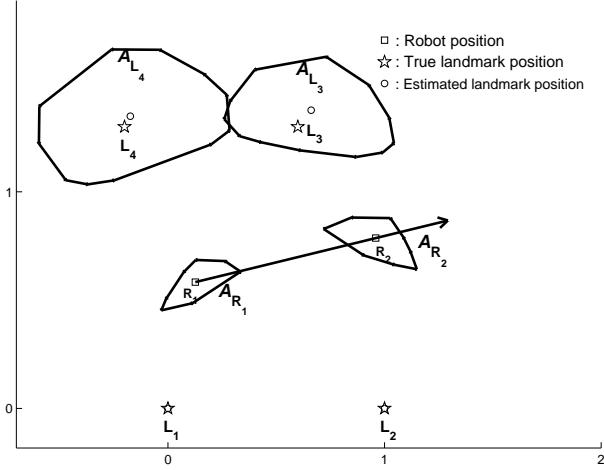


Figure 6: The uncertainty regions in \mathcal{F}_L are derived from the uncertainty regions in \mathcal{F}_R (see Figure 2). The centroids of the uncertainty regions are used to estimate the positions of the different objects. The areas of the polyhedra quantify how uncertain the estimates are.

In other words, the uncertainty region \mathcal{A}_{R_j} of the robot position in \mathcal{F}_L is

$$\bigcup_{h_1 \in \mathcal{A}_{L_1}, h_2 \in \mathcal{A}_{L_2}} \mathcal{T}_{(h_1, h_2)}(X_R(R_j)) \quad (5)$$

The uncertainty regions \mathcal{A}_{L_i} for L_3 and L_4 in \mathcal{F}_L are computed similarly,

$$\bigcup_{h_1 \in \mathcal{A}_{L_1}, h_2 \in \mathcal{A}_{L_2}} \mathcal{T}_{(h_1, h_2)}(X_R(\mathcal{A}_{L_i})) \quad (6)$$

In practice, we consider the convex hull of the images of the vertices of the polyhedra in \mathcal{F}_R . In this example, we take the four vertices (the extreme points) L_1^k and L_2^k (where $k = 1 \dots 4$) from \mathcal{A}_{L_1} and \mathcal{A}_{L_2} . The number of possible combinations of L_1^k and L_2^k is here 4^2 . In \mathcal{F}_L , the polyhedron \mathcal{A}_{R_j} approximates the set of all consistent points for R_j . The number of possible vertices for \mathcal{A}_{L_3} in \mathcal{F}_L is 4^3 . This is because of the uncertainty region of L_3 in \mathcal{F}_R is a polyhedron with 4 vertices.

Figure 6 shows the estimated uncertainty regions of R_1 , R_2 , L_3 and L_4 in \mathcal{F}_L .

We have tested the proposed method both in simulation and on a real robot. These results are presented in the next sections.

3.2 Simulation

We tested the proposed method in simulation in an environment with four landmarks (at unknown positions to the localization system). The robot moves in a polygonal line around the centre with some randomness. Since we focus on landmark initialization, Figure 7 shows only the estimated positions of the landmarks.

Two landmarks are arbitrarily selected as L_1 and L_2 . With the change of frames from \mathcal{F}_R to \mathcal{F}_L , the uncertainty regions \mathcal{A}_{L_3} and \mathcal{A}_{L_4} (two polyhedra) are computed. When another pair of observations is available (after the robot has moved again), new \mathcal{A}_{L_3} and \mathcal{A}_{L_4} can be obtained in the same manner. The estimated positions from all movements are unifiable since they are with respect to the same frame \mathcal{F}_L . Figure 7 shows how the uncertainty regions are refined after several movements by computing the intersection of the sequence of polyhedra. The polyhedra \mathcal{A}_{L_3} and \mathcal{A}_{L_4} shrink gradually. A global map with the estimated positions and the corresponding uncertainty regions of all landmarks is incrementally built this way.

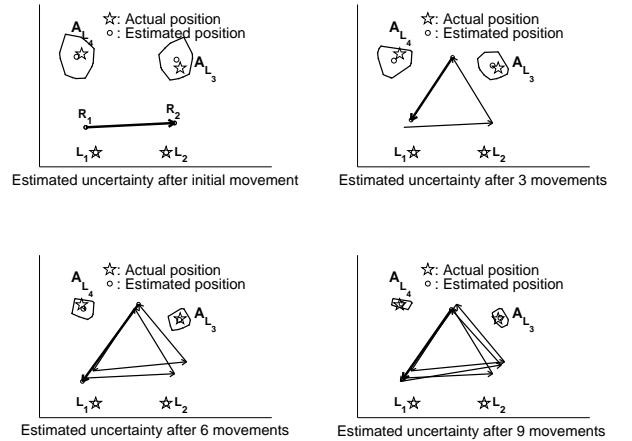


Figure 7: \mathcal{A}_{L_3} and \mathcal{A}_{L_4} gradually shrink as the number of observations increases. The arrows represent the robot movements.

4 Evaluation on a Real Robot

Our localization technique was evaluated using a Khepera robot. The Khepera robot has a 5 centimetre diameter and is equipped with a color camera (176 x 255 resolution). A kheperaSot robot soccer playing field, 105 x 68 square centimetres, was used as the experimental arena. There were four artificial landmarks in the playing field. Only one landmark

was distinguishable from the others. The second landmark was placed 20 centimetres apart from the first landmark as shown in Figure 8.



Figure 8: Environment for the real robot experiments.

During the experiments, the robot moves in a polygonal line by alternating panoramic view taking, on the spot random rotation, and motion in straight line. Landmark bearings were extracted from the panoramic images using a color thresholding technique. Bearings from any two consecutive observations were used to estimate the landmark locations as described in [Huang *et al.*, 2005].

The vision error ϵ is limited to ± 2 degrees. Figure 9 shows the estimated landmark positions after 10 pairs of observations. The actual landmark positions are denoted by stars, the estimated landmark positions are shown as circles, and the areas of the polyhedra represent the uncertainty regions.

The uncertainty regions of the third and fourth landmarks decreases rapidly in the first few observations and does not change much after the third observation as shown in the top chart of Figure 10. The bottom chart of Figure 10 displays the distances from the estimated landmark positions to the actual landmark positions. The estimated errors of third landmark and fourth landmark are 2 centimetres and 3 centimetres respectively from the actual positions. The unit length equals to 20 centimetres. Figure 10 shows that the estimated error might increase if the centre of new uncertainty region is apart

from the actual landmark position as in the case of third landmark.

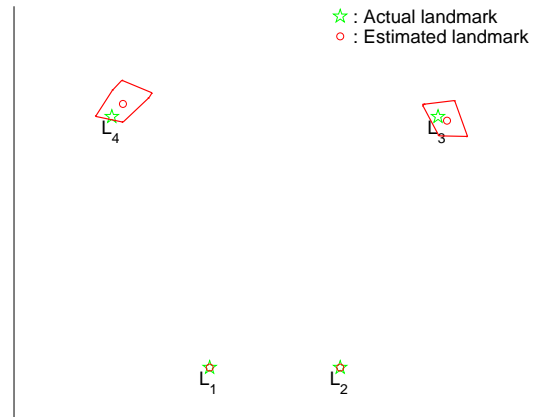


Figure 9: Estimated landmark positions after performing 10 observations

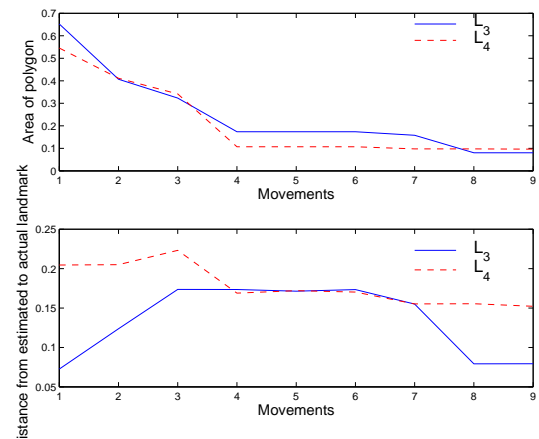


Figure 10: Uncertainty regions of 3rd and 4th landmarks

In this system, the only parameter is the maximum degree of vision error ϵ . To study the effect of this parameter, the sizes of the uncertainty regions computed by the system given a same bearing set but different values of ϵ were compared. The robot collected the landmark bearings by repeating the same random trajectory 10 times. The ϵ was varied from 2 to 7 degrees. Figure 11 shows the relation between the level of vision error ϵ , and the uncertainty area of the third landmark. The areas of uncertainty were affected by the level of ϵ in a linear manner.

5 Discussion and Future Work

In this paper, we have introduced a method for analysing how uncertainty propagate when information is transferred from one observer attached to a robot frame to an observer attached

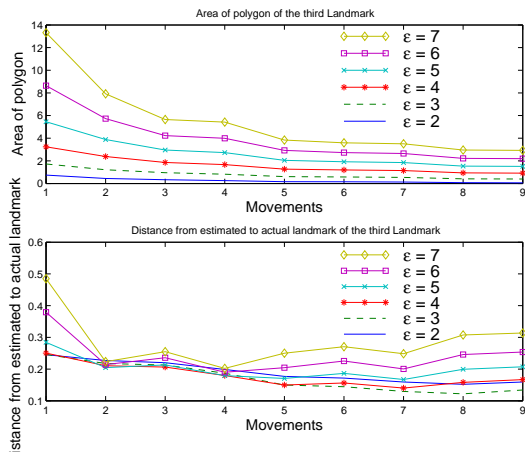


Figure 11: Uncertainty at different level of maximum vision error, ϵ

to a landmark frame. The method was demonstrated both in simulation and on a real robot. In future work, we will address the problem of inconsistent observations. This will be done by using the uncertainty cones in a voting mechanism to compute the likelihood of the objects in the environment. In other words, union of polyhedra will be used to represent probability density functions.

References

- [Bailey, 2003] T. Bailey. Constrained initialization for bearing-only slam. *IEEE International Conference on Robotics and Automation*, 2003.
- [Costa *et al.*, 2004] A. Costa, G. Kantor, and H. Choset. Bearing-only landmark initialization with unknown data association. In *Proceedings of the 2004 IEEE International Conference on Robotics and Automation*, volume 2, pages 1764 – 1770, 2004.
- [Davison *et al.*, 2004] A. Davison, Y. Cid, and N. Kita. Real-time 3d slam with wide-angle vision. *IAV2004 - PREPRINTS 5th IFAC/EURON Symposium on Intelligent Autonomous Vehicles Instituto Superior Tecnico, Lisboa, Portugal July 5-7, 2004*, 2004.
- [Davison, 2003] A. Davison. Real-time simultaneous localization and mapping with a single camera. In *Proceedings of International Conference on Computer Vision, Nice, October, 2003*.
- [Delahoche *et al.*, 1997] L. Delahoche, C. Pegard, B. Marhic, and P. Vasseur. A navigation system based on an omni-directional vision sensor. In *Int. Conf. on Intelligent Robotics and Systems*, pages 718–724, 1997.
- [Dissanayake *et al.*, 2001] G. Dissanayake, S. Clark, P. Newman, H. Durrant-Whyte, and M. Csorba. Estimating uncertain spatial relationships in robotics. *IEEE Transactions on Robotics and Automation*, 17(3):229 – 241, 2001.
- [Huang and Maire, 2004] H. Huang and F. Maire. A localization system solely based on vision for autonomous lawnmowers. In *Proceedings of the 2004 International Conference on Computational Intelligence for Modelling, Control and Automation*, pages 657 – 663, 2004.
- [Huang *et al.*, 2005] H. Huang, F. Maire, and N. Keeratiprannon. A direct localization method using only the bearings extracted from two panoramic views along a linear trajectory. *Autonomous Minirobots for Research and Education, AMiRE2005, in press. Fukui, Japan, 2005*.
- [K. Usher and Corke, 2002] P. Ridley K. Usher and P. Corke. Visual servoing of a car-like vehicle - an application of omnidirectional vision. In *Proceedings of 2002 of Australian Conference on Robotics and Automation, Auckland, 2002*.
- [Kwok and Dissanayake, 2004] N. M. Kwok and G. Dissanayake. An efficient multiple hypothesis filter for bearing-only slam. In *Proceedings of 2004 IEEE/RSJ International Conference on Intelligent Robots and Systems*, 2004.
- [Kwok *et al.*, 2004] N. M. Kwok, D. K. Liu, G. Fang, and G. Dissanayake. Path planning for bearing-only simultaneous localization and mapping. In *Proceedings of the 2004 IEEE Conference on Robotics, Automation and Mechatronics. Singapore, 1-3 December, 2004*.
- [Lemaire *et al.*, 2005] Thomas Lemaire, Simon Lacroix, and Joan Sola. A practical 3d bearing-only slam algorithm. available at: <http://www.comets-uavs.org/papers/LEMAIRE-IROS-2005.pdf>, 2005.
- [Leonard and Durrant-Whyte, 1991] J. J. Leonard and H. F. Durrant-Whyte. Simultaneous localization for an autonomous mobile robot. In *in Proc. IEEE/RSJ on Intelligent Robots and System, Osaka, Japan, 1991*.
- [Montemerlo and Thrun, 2003] M. Montemerlo and S. Thrun. Fastslam 2.0: An improved particle filtering algorithm for simultaneous localization and mapping that provably converges. In *Proceedings of the International Joint Conference on Artificial Intelligence*, 2003.
- [Rizzi and Cassinis, 2001] A. Rizzi and R. Cassinis. robot self-localization system based on omni-directional color images. In *Robotics and Autonomous Systems 34*, pages 23–38, 2001.
- [RoboMower, 2005] RoboMower. Website of the commercial lawnmower called robomower. <http://www.friendlyrobotics.com>, 2005.
- [Russell and Norvig, 2003] S. Russell and P. Norvig. *Artificial Intelligence - A Modern Approach*. Prentice Hall, Upper Saddle River, New Jersey, 2003.

- [Siegwart and Nourbaksh, 2004] Roland Siegwart and Il-lah R. Nourbaksh. *Introduction to Autonomous Mobile Robots*. The MIT Press, Cambridge, Massachusetts; London, England, 2004.
- [Smith *et al.*, 1990] R. Smith, M. Self, and P. Cheeseman. Estimating uncertain spatial relationships in robotics. *Autonomous robot vehicles*, pages 167–193, 1990.
- [Sola *et al.*, 2005] Joan Sola, Andre Monin, Michel Devy, and Thomas Lemaire. Undelayed initialization in bearing only slam. available at: <http://www.laas.fr/~jsola/papers/undelayedBOSLAM.pdf>, 2005.
- [Toro, 2005] Toro. Website of the commercial lawnmover called toro. <http://www.toro.com>, 2005.
- [Yagi *et al.*, 1998] Y. Yagi, M. Fujimura, and M. Yashida. Route representation for mobile robot navigation by omnidirectional route panorama transformation. In *Proceeding of the IEEE International Conference on Robotics and Automation, Leuven, Belgium*, 1998.
- [Zunino and Christensen, 2001] G. Zunino and H. I. Christensen. Simultaneous localization and mapping in domestic environments. In *in Proc. Intl. Conf. on Multisensor Fusion and Integration for Intelligent System*, 2001.